

Quark-Matter 2006

Fluid Dynamics as Diagnostic Tool for Heavy Ion Collisions

Björn Bäuchle^{1,2}, Yun Cheng¹, László P Csernai^{1,3,†},
Volodymyr K Magas⁴, Daniel D Strottman⁵, Péter Ván^{1,3}
and Miklós Zétényi¹

¹ Section for Theoretical Physics, Departement of Physics, University of Bergen, Allégaten 55, 5007 Bergen, Norway

² Institut für theoretische Physik, Universität Frankfurt, Max-von-Laue-Straße 1, D-60438 Frankfurt am Main, Germany

³ KFKI Research Institute for Particle and Nuclear Physics, P.O. Box 49, 1525 Budapest, Hungary

⁴ Departament d'Estructura i Constituents de la Matèria, University of Barcelona, Av. Diagonal 647, 08028 Barcelona, Spain

⁵ Theory Division, Los Alamos National Laboratory, Los Alamos, NM, 87454, USA

E-mail: csernai@ift.uib.no, baeuchle@th.physik.uni-frankfurt.de

Abstract.

Ultra-Relativistic Heavy Ion Collisions at an energy $\sqrt{s_{NN}} = 65$ GeV are studied in a three-dimensional Fluid Dynamical model. The results of a hydrodynamical evolution using the PIC-method are shown. The importance and diagnostic value of a proper reaction plane determination is emphasized, and the time development of collective observables is presented.

PACS numbers: 24.10.Nz, 25.75.-q

Submitted to: *J. Phys. G: Nucl. Part. Phys.*

Introduction: Fluid Dynamical (FD) models are widely used to describe ultra-relativistic heavy ion collisions. Their advantage is that one can vary flexibly the Equation of State (EoS) of the matter and test its consequences on the reaction dynamics and the outcome. In energetic collisions of large heavy ions, especially if QGP is formed in the collision, one-fluid dynamics is a valid and good description for the intermediate stages of the reaction. Here, interactions are strong and frequent, so that other models have limited validity. On the other hand, the initial and final, Freeze-Out (FO), stages of the reaction are outside the domain of applicability of the fluid dynamical model.

The equations of perfect FD are just the local energy, momentum and baryon number conservation laws, where we assume local equilibrium, so that the energy-momentum tensor is given by the EoS. Thus, the most important and almost only input is the EoS.

† Speaker

Of course the initial and final (FO-) conditions are also vital, and the deviations from thermal equilibrium (viscosity and dissipation) are also important. Here, though, we will concentrate on the impact of the initial condition.

As pointed out above, the equations of perfect hydrodynamics are the conservation laws. Still, the approach additionally assumes a local thermal equilibrium. If this is present, intensive macroscopic space-dependent quantities such as temperature, T , chemical potential, μ_B , and pressure, P , can be defined. An Equation of State has to be introduced, which gives a relationship between energy- and baryon number density and the pressure: $P = P(e, n)$. This is necessary to have a complete, solvable set of equations. After introducing the shear viscosity, η , and the heat conductivity, κ , a state near equilibrium can also be described.

The PIC Model: The Particle in Cell (PIC) method was developed by Amsden and Harlow in the early 1960s [1] and upgraded to ultra-relativistic energies by Nix and Strottman in the 80s and 90s [2]. The method takes advantage of a combination of Eulerian and Lagrangian solution methods; the pressure is calculated on an Eulerian grid, while all current transfers are calculated in a larger number of Lagrangian cells, the so-called “marker particles”.

The method has numerous advantages (e.g. keeping conserved quantities constant), and a typical main disadvantage, the development of “ringing instabilities” in rapid expansion or explosion. This has recently been eliminated by assigning the marker particles random positions to avoid structures, along which an instability would start to develop. With this upgrade the stability of expansion is increased, so that a spherical object remains exactly spherical (within the numerical resolution) even after a volume increase by a factor of more than 100.

After upgrades, the code can follow the fluid dynamical expansion even well beyond the physical applicability of FD. This extended FD history can then be used to analyse the effects of choices on the FO hyper-surface, or on the FO layer (a 4-volume domain).

A code with finite cell-size exhibits necessarily a numerical viscosity and coarse graining. The kinetic energy lost in this averaging is thermalized just as in nature. No additional constraint is enforced to conserve the entropy.

The numerical viscosities are in the range of the estimated physical viscosity [3], if the reaction is not too peripheral, in which case the applicability of FD is not the best anyway. The larger than realistic viscosities in the transverse direction dissipate more transverse flow to heat, so we get higher T and higher thermal smearing.

The initial State: The initial shape is calculated in an effective 1D Yang-Mills coherent field model, where the transverse plane is split up to “streaks” like in the “Firestreak”-model of the 1970s [4, 5]. Projectile and target matter interpenetrate each other initially in the collision, exchange color charge and form “strings” which expand until all initial kinetic energy is converted to string tension. No transverse momentum exchange is taken into account among the streaks in this initial stage, but a longitudinal expansion at the edges of the strings was included in the expansion to make the surface at the initial moment (when the FD starts) smoother.

The streaks expand until the initial kinetic energy is converted fully into string tension. We use an effective string tension of $6 - 8 \text{ GeV/fm}$, which was deduced from earlier string model fits to experimental CERN - SPS results. This results in

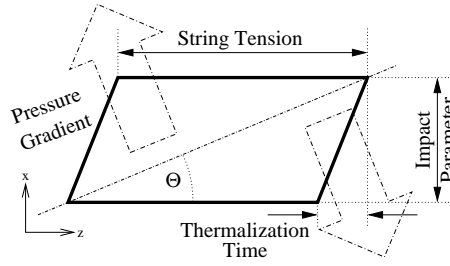


Figure 1. A schematic view on the initial state of a heavy ion collision as used in PIC. The labeled lengths indicate the dependence on the particular quantity, not the quantity itself.

moderately long streaks of 4 – 8 fm, so that the thickness of the initial state is rather a flat than an extremely long object parallel to the beam direction.

While in the middle of the transverse plane in the CM frame the matter is at rest, the edges on the projectile and target side have projectile- and target-directed excess momenta, which lead to a skewed object at the end of the initial state. The longer the formation of initial state lasts, the more skewed this initial state becomes (figure 1).

Non-existing Symmetry and Event-plane reconstruction: Although both nuclei involved in the collision of two gold beams are of equal size and mass, there is no forward-backward (F/B)-symmetry. In each event a clear distinction between projectile and target hemisphere must be made. It is trivial to see that a single-event particle distribution following from an initial state of finite impact parameter as described above, is not F/B-symmetric but deviates from this by a certain angle Θ in the x/z-plane (see figure 1). If the event-plane reconstruction is not done for its F/B-orientation, these effects are lost.

The aforementioned effect, the *third flow component*, has been predicted as a signature of the QGP [6, 7]. It should be visible in the special behaviour of the directed flow coefficient $v_1(y)$, which is supposed to be closer to zero at central rapidities than the usual linear increase of v_1 vs. rapidity, y . This effect is measurable at around midrapidity [8]

Especially correlation measurements, but also flow determinations, must be aware of this fact. Two-particle correlations showing basically two peaks at $\Delta\eta = 0$ and $\Delta\phi = 0, 2\pi$ do not take the real geometry into account. Taking a sample over events with randomly identified F/B event planes obscures the advent of interesting physics.

Results: The distorted initial state has the biggest pressure gradient along the lines indicated in figure 1. This leads to a distribution of matter and energy density in an ellipsoid shape in very late stages of the collision, which is enhanced in the direction of the original pressure gradient. Figure 2 shows the calculated energy-density in the x/z-plane after 8 (a) and 71 (b) cycles, respectively (corresponding to times $t_1 = 0.3$ fm/c and $t_2 = 2.7$ fm/c after the beginning of the hydro-evolution). The flow patterns that follow from the initial state can be seen in figure 3. The presence of the third flow component is well visible in the former. It can also be seen that both directed and elliptic flow coefficients approximately double their magnitude between the two times.

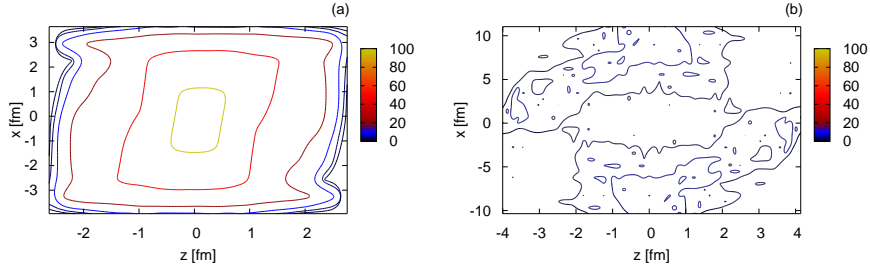


Figure 2. (Color online) The energy-density in the $y = 0$ - plane at two different times (after 0.3 fm/c (a) and 2.7 fm/c (b)) in Au+Au-collisions at $\sqrt{s_{NN}} = 65$ GeV at impact parameter $b = 0.7 (R_1 + R_2)$. Note different scales between the plots.

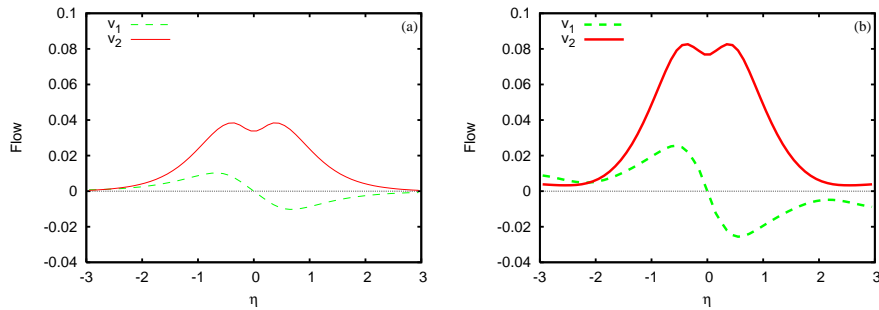


Figure 3. (Color online) The flow coefficients v_1 and v_2 as a function of pseudorapidity η at two different times (after 0.3 fm/c (a) and 2.7 fm/c (b)) in Au+Au-collisions at $\sqrt{s_{NN}} = 65$ GeV at impact parameter $b = 0.7 (R_1 + R_2)$.

All flow plots are calculated assuming massless quarks in a QGP-Phase. In evaluating the flow during the hydro evolution we take advantage of the observed N_q -scaling. It should further be noted that all flow plots are calculated at constant time hypersurfaces. This is of course not including freeze-out and hadronization, but it allows us to study effects of different initial conditions during the hydro evolution. This leads to a larger v_1 than in experimental data [8], because, we neither performed a FO calculation through a realistic FO hypersurface, nor an impact parameter averaging. Both these processes make the distributions smoother and decrease v_1 and v_2 . The “dip” in v_2 at midrapidity is a consequence of too small numerical viscosity in longitudinal direction.

Acknowledgements: This work is supported by the Computational Subatomic Physics project of the Research Council of Norway and by the Hadron Physics EU Integrated Infrastructure Initiative.

References

- [1] A. A. Amsden and F. H. Harlow *J. Comp. Phys* **3** 1 (1968) 94-110 and A. A. Amsden, A. S. Goldhaber, F. H. Harlow and J. R. Nix, *Phys. Rev. C* **17** (1978) 2080.
- [2] R. B. Clare *et al* *Phys. Rept.* **141** (1986) 177, D. Strottman, *Lecture Notes in Mathematics* 1385: (1989) 278-289 and N. S. Amelin *et al* *Phys. Lett. B* **261** 4 (1991) 352-356
- [3] L. P. Csernai, E. Molnar, A. Nyiri and K. Tamosiunas, *J. Phys. G* **31** (2005) S951.
- [4] V. K. Magas, L. P. Csernai and D. D. Strottman, *Phys. Rev. C* **64** (2001) 014901
- [5] V. K. Magas, L. P. Csernai and D. Strottman, *Nucl. Phys. A* **712** (2002) 167
- [6] L. P. Csernai and D. Rohrlich, *Phys. Lett. B* **458** (1999) 454
- [7] L. P. Csernai *et al.*, *Acta Phys. Hung. A* **22** (2005) 181
- [8] G. Wang, arXiv:nucl-ex/0701045.